RSC Advances

Removal of ciprofloxacin from Aqueous Solution on Long TiO$_2$ Nanotubes with High Specific Surface Area

Kai Zheng[a], Xingye Zheng[a], Fei Yu[c], Jie Ma[b*]

[a]Department of Environmental Engineering, Nanjing Institute of Technology, Nanjing, 211167, P. R. of China.

[b] State Key Laboratory of Pollution Control and Resource Reuse, School of Environmental Science and Engineering, Tongji University, 1239 Siping Road, Shanghai 200092, P. R. of China. Tel: 86-21-6598 1831;

c College of chemistry and environmental engineering, Shanghai Institute of Technology, Shanghai 2001418, P. R. of China. Tel: 86-21- 60873182

Abstract：The long TiO$_2$ nanotubes (TN) were successfully prepared by reaction TiO$_2$ and NaOH. The raw underwent following procedures:stirring, ion exchange, centrifugation, and freeze-drying, and then the target product TN was synthesized sucessfully. The anatase TN was obtained by calcinating TN at 823 K for 4.5 h. The characteristic of TN was performed by means of BET (Brunauer, Emmett and Teller), X-ray Diffraction (XRD), scanning electron microscope (SEM), transmission electron microscope(TEM), and X-ray photoelectron spectrum (XPS). The results indicated that the TN exhibited larger specific surface area (~160 m^2/g) and pore volume (~0.6 cm^3/g) than those of commercial product P25. The adsorption performance of ciprofloxacin (CIP) onto TN was evaluated,the commercial product P25 was chosen as comparison target. The adsorption isotherm, kinetic and regeneration performance were investigated. The experimental results indicated that maximum adsorption capacity of TN and P25 were 26.38 and 5.32 mg/g, respectively, their adsorption behaviors are better fitted with Langmuir model than

23   Freundlich model. Kinetic regression results shown that the adsorption kinetic was more accurately

24   represented by a pseudo second-order model than pseudo-first-order model, reaction rate values of

25   pseudo-second-order on P25 and anatase TN were 0.0442 and 0.27463 min^{-1}, respectively. After

26   adsorption process, TN represented better regeneration properties than P25 under the irradiation lamp

27   with 500 watts for 3 h in 5 ml aqueous solution. Above analysis results further certified that long TN

28   exhibited better adsorption capacity and regeneration properties than that of P25. This study provides a

29   green method for the removal of organic pollutants by combining adsorption enrichment with

30   photocatalytic degradation.

31

32   **Keywords:**Ciprofloxacin; Long TiO_2 Nanotubes; Adsorption; Regeneration; Photo-catalysis;

Introduction

Ciprofloxacin(CIP) as a broad-spectrum quinolone antibacterial drugs antibiotic, it has been widely used in human and veterinary medicine[1]. Lately, CIP has been availed of feeding poultry to guard them against disease during their growth period. Fluorinated functional groups in CIP are incompletely metabolized, and existed in the state with drug activity[2, 3]. In European approximately more than ten thousands tons of antibiotics were consumed in 1999, farming animals and therapeutic drugs accounted for 35% and 29%, respectively, which has decreased by 50% since 1997. Because of CIP can not be completely decomposed, the persistent release of CIP into the environment made it exhibit similar exposure characteristics with chemicals difficult to degrade[4]. CIP with concentrations from ng/L to µg/L has been detected in surface waters and effluent-dominated systemsin the U.S.[5], Canada[6-8], and Europe [9-12].

The detection of CIP in the atmosphere, water and soil arouses human beings to care about health issues. More importantly, wastewater containing CIP was discharged into aquatic environments, so antibiotic resistance can be gradually formed within native bacterial populations. From the point of annual sales and variability of thedrug, fluoroquinolones is one of the most important types of antibiotics [13, 14]. They are effective in resisting all kinds of bacteria and could regard as final medicine for remedy. CIP belongs to derivatives with fluoroquinolone groups and is a principalmetaboliteof enrofloxacin. CIP is present of different states depending on solution pH. The main species of CIP include three forms: negative ion, positive ion, or amphoteric ion. The existing state of CIP can affects many performances, such as soil adsorption, its photolysis, and reactive activity on targets[15-17].

Recently, adsorption and photo-catalytic technology have been widely utilized by scientists to remove CIP from aqueous solution. One of the merits of adsorption was its low cost. However, the whole

55   sorption process is incomplete due to the heterogeneity from adsorbents and the difficulty to completely

56   decompose. Adsorbed CIP was widely found in treatedwater body and occurrence of CIP in Italian

57   STPs[18]. Furthermore, CIP adsorbed to land-applied adsorbents can not be efficiently and fast decomposed

58   and thus may still be released into receiving water body via exogenic action. As adsorbents have a finite

59   capacity for pollutant molecules, it is necessary either to regenerate or dispose of them.

60   Photocatalytic oxidation of organic pollutants is often carried out, the photocatalytic activity depends

61   on the ability of the catalyst to create electron-hole pairs, which generate free radicals (e.g. hydroxyl

62   radicals: •OH) able to undergo secondary reactions. However, photocatalytic oxidation technology have

63   not been widely applied in the practical wasterwater treatment, the following existing problems

64   associated with removal pollutants by photocatalytic oxidation of TiO_2 included some disadvantages：

65   existing particles and chrominance from the pollutants causing refraction, reflection and scattering of

66   light; catalytic speed of photocatalyst is much greater than the adsorption and diffusion speed, and lead to

67   the more electron-hole pair recombination during photocatalysis, hence, traditional photocatalyst of TiO_2

68   and photocatalytic technology exist lower catalytic efficiency, higher energy consumptionm, and high

69   operation cost[19]. It would be very attractive to extend the application of photocatalytic oxidation

70   technology to the removal of organic pollutants, but still a challenge.

71   In this paper, we convert the traditional adsorption-catalysis process into two seperated process,

72   polluants firstly enriched on the adsorbents and then put adsorbents in the clear water to catalyze after

73   preferential adsorption. This technology concentrated pollutants firstly and facilitated pollutant

74   mineralization process so that the catalyst or adsorbents be regenerated, and then contaminants can be

75   removed through mineralization reaction.

76   Many synthesis routes to the various morphologies and crystallite phases of TiO_2 have been reported

77   in the literature. Among the most commonly used are solution methods: sol-gel[20], hydrothermal[21],

78   solvothermal[22], anodic oxidation[23], hard template[24], and direct oxidation[25]. Recently, titanium dioxide

79   was used for the degradation of CIP by utilizing its photocatalysis property under the ultraviolet light

80   irradiation[26]. However, the surface area and pore volume of commercial TiO_2 are respectively about 50

81   m^2/g and 0.1 cm^3/g, lower surface area and pore volume restrict its adsorption application, thus limit its

82   catalyzing performance. To overcome above-mentioned shortcomings, the structure of TiO_2 must be

83   improved to enhance its adsorption capacity and catalyzing efficiency.

84   Recently, scientists have developed TiO_2 nanotubes to improve its catalytic performance, among the

85   most commonly used as following: crystallizing amorphous anodized TiO_2 nanotubes at low

86   temperature[27]; electrochemical etching and hydrothermal synthesis method[28]; NaOH treatment of TiO_2

87   particles[29]; However, these procedures generally involve inherent drawbacks including time-consuming,

88   complicated, and expensive processes that are not industrially viable. Costeffective, large-scale

89   preparations of stable, high surface area, mesoporous TiO_2 need to be developed.

90   In this paper, we report a protocol to synthesize long TiO_2 nanotube(TN) with high surface area(160

91   m^2/g) by a stirring hydrothermal method. The mechanical force-driven stirring process synchronously

92   improving the diffusion and surface reaction rate of titanate nanocrystal growth in solution phase, is the

93   reason for lengthening the titanate nanotubes. The TN exhibiated outstanding adsorption performance due

94   to its larger specific surface area (SSA) and it can be utilized to efficiently adsorpt and remove the

95   pollutants. Besides, TN used as adsorbent with excellent catalyzing performance can be availed of

96   implementing both mineralization the pollutants and regenration of adsorbent. The above method provide

97   a effevtive approach for efficient removal of pollutants.

98

2. Experimentals

2.1. Materials and chemicals

All chemicals were purchased from Sinopharm Chemical Reagent Co., Ltd (Shanghai, China) in analytical purity and used in the experiments directly without any further purification. All solutions were prepared using deionized water.

2.2 Preparation of TiO_2 and TN

The 25 g $TiCl_4$ (purity 99%) was added to 2 L demonized water with 2 ml concentrated sulfuric acid. After the $TiCl_4$ was completely hydrolyzed, about 120 to 140 ml 17% ammonia was drop wise added to ensure the mixture pH value between 7.0 and 7.5. The raw mixture was filtrated and rinsed with deionized water to remove NH_4Cl until the leaching liquid could not produce white precipitation with 0.2 mmol/L Ag_2SO_4. The filtrated residue successively underwent desiccation at 373 K for 2 h and vacuum drying at 353 K under pressure of 10^{-1} Pa for 3 h, and then $Ti(OH)_4$ was achieved. The anatase crystal form TiO_2 was achieved by incinerating $Ti(OH)_4$ at 823 K for 4.5 h.

3 g anatase titanium dioxide was added to 350 ml 10mol/L sodium hydroxide solution, then the mixture was stirred with ultrasound for 2 h afterwards with magnetic stirring at 200 revolutions per minute(rpm) for 2 h. The solution mentioned above and a magnetic rotator were together added into Teflon reactor with 500 ml volume. The reactor was put into the heater with a magnetic stirring apparatus (RCT basic, IKA Corporation, Genmany). The reactor was operated with needed mixed speed (about 600 rpm) at 403 K for 20-24 h.

The product, sodium titanate, was obtained by centrifugation. and then rinsing five times until the pH of washing solution equivalent to 11, then 0.5 mol/L hydrochloric acid was in batches added to adjust the pH of solution equivalent to 2, this condition maintained 3 to 4 h to make the adequately exchange

121 between hydrogen ion and sodion in solution. Above mixture was rinsed about five times until the pH of

122 washing solution equivalent to 6.8-7.0 and filtrated, generating the hydrogen titanate nanotube materials.

123 The residue was treated under vacuum free-drying. The crystal of long TiO_2 nanotubes was achieved at

124 823 K for 4.5 h. In the end, the product of long TiO_2 nanotubes was acquired and abbreviated as TN.

125 2.3 Batch adsorption experiments

126   CIP concentration was determined colorimeterically by measuring at maximum absorbance

127 (λ_{max}=275 nm). A calibration curve was plotted between absorbance and concentration of the CIP to

128 obtain the absorbance-concentration profile of the CIP based on Beer-Lambert's law. For high

129 concentration CIP, dye samples were diluted before absorbance measurements. The concentration of the

130 CIP in the solution was determined by the Beer-Lambert's law expression[30]. Batch adsorption

131 experiments were conducted in 50 ml glass bottles with 20mg adsorbents and 40 ml CIP solution of

132 different initial concentrations of 5~50 mg/L, and the pH of the solution was adjusted to ~7.0 (nearly in

133 neutral solution to avoid the unpredictable influence) with HCl or NaOH solutions. Timing of the

134 sorption period started as soon as the solution was poured into the bottle. Sample bottles were shaken on a

135 shaker (TS-2102C, Shanghai Tensuclab Instruments Manufacturing Co., Ltd., China) and operated at a

136 constant temperature of 25 °C and 150 rpm for 24 h to achieve adsorption equilibrium. All adsorption

137 experiments were conducted in duplicate, and only the mean values were reported. The maximum

138 deviation for the duplicates was usually less than 5%. After adsorption equilibrium has been achieved, the

139 CIP concentrations of the solutions were measured using a spectrophotometer (UV759UV-VIS, Shanghai

140 Precision &Scientific Instrument Co. Ltd.). Kinetic studies were performed at a constant temperature of

141 25 °C and 150 rpm with 25(P25) and 50(TN) mg/L initial concentration of CIP solutions.

142   The amount of adsorbed CIP on adsorbents (q_t, mg/g) was calculated as follows:

143
$$q_t = (C_0 - C_t) \times \frac{V}{m} \tag{1}$$

144   where c_0 and c_t are the CIP concentrations at the beginning and after a period of time (mg/L), V is

145 the initial solution volume (L); and m is the adsorbent weight (g).

146 2.4 Regeneration studies

147   After adsorption, TN and P25 adsorbents were placed in a quartz pot in a black box under UV light

148 with a 500 W ultraviolet lamp for 3 h. The samples were rinsed with distilled water, and then the samples

149 were dehydrated by freeze-drying. The adsorption experiments of the obtained samples were conducted

150 as the first regeneration cycle adsorbent. The above process was repeated 6 times to study the ability of

151 the photocatalytic technology to regenerate the adsorbents.

152 2.5 Characterization methods

153   The surface morphologies of samples were visualized using field-emission scanning electron

154 microscopy (SEM, Hitachi S-4800), operating at a typical accelerating voltage of 10 kV. The

155 microstructure and morphology of samples were analyzed using high-resolution transmission

156 electron microscopy (JEM 2100F, accelerating voltage of 200 kV, JEOL).The existing state of

157 related atoms belonging to examined substance, X-ray photoelectron spectroscopy (XPS) analysis was

158 operated in a Kratos Axis Ultra DLD spectrometer, sing monochromatic Al/Ka X-rays, at a base pressure

159 of 1×10^{-9} Torr. Unico UV2100 spectrophotometer was employed to analyzing the CIP concentration at a

160 wave length of 275 nm.

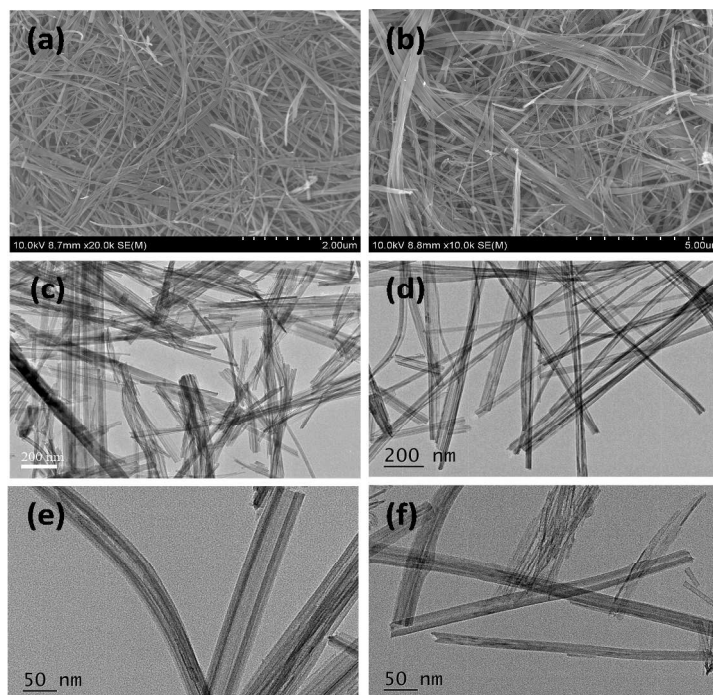161 **3. Results and discussion**

162 3.1 The characterization of TN

163

Fig.1Typical SEM (a, b) and TEM images (c, d,e,f) of TN

165   As shown in Fig.1, the TiO_2 powder was transformed into elongated nanotubular structure. During the

166   whole reaction, the TiO_2 dissolved in NaOH solution had been converted into sodium titanate. The

167   saturated sodium titanate can form crystal. The saturated sodium titanate was vigorously stirred, which

168   produced centrifugal force and shearing force, the centrifugal force and the stirring speedshowed linear

169   relationship, meantime the shearing force and stirring speed showed curve relationship; thus the diameter

170   of TN is closely related to centrifugal force, the length of TN is closely relative to shearing force. Thus

171   structure of TN can be effectively controlled by optimizing experimental parameters (temperature, time,

172   mixing speed, post-treatment method of raw materials). It can be seen from Fig. 1e and Fig. 1f that the

173   length of prepared anatase TN was ranged from1.0 μm to 2 μm, which is longer than the previous reports,

174   as shown in Table S1, and TN had the hollow tube shape in the middle of TN.

175

176
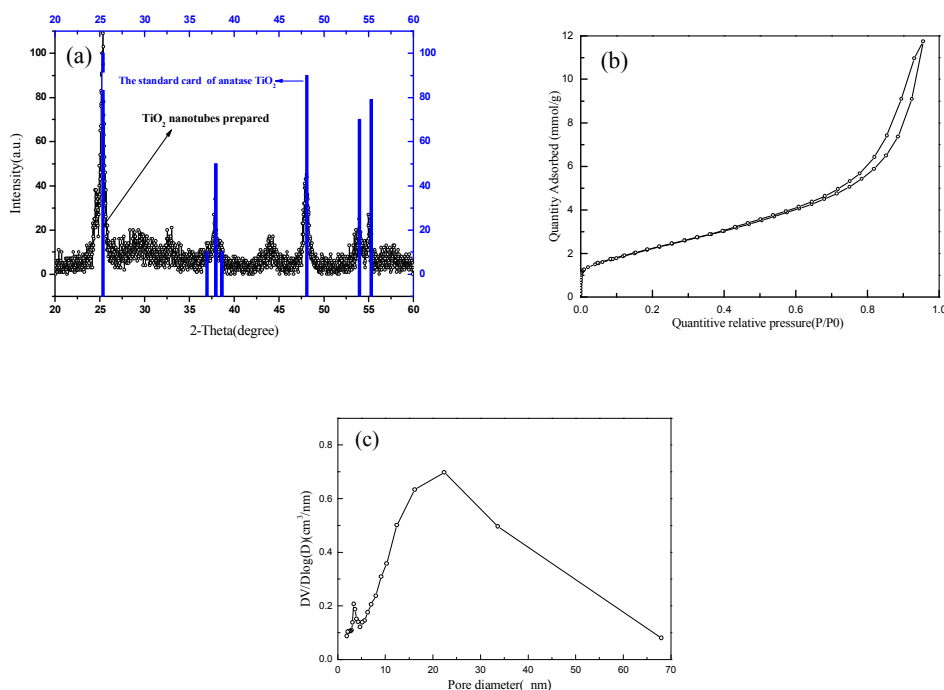
Fig. 2 XRD patterns (a), adsorption and desorption isotherm (b) of N_2, and pore diameter distribution

(c) of TN

As can be seen from Fig.2a，prepared TN appeared single and strong peak at maximum diffraction

angles at 25.3° and 48.2°; triple peak at 36.9°, 37.8° and 38.61°; double and medium peak at 54° and

55.3°. It can be obviously observed that the characteristics that TN were almost the same as those of the

anatase TiO_2 standard card (PDF#00-002-0387). Such results further indicated that prepared anatse TN

was of anatase crystal form. As can been seen from Fig. S1 that sodium titanate exhibited strong peaks at

about 10° attributed to titanate. The results showed that peaks at about 10° were weaker when sodium

titanate have exchanged with hydrogen ion, this phenomenon confirmed that sodium titanate had been

converted into titanium dioxide. The results from Fig. S1 indicated that crystalline form of incinerated TN

at 823 K for 4.5 h belonged to anatase. Experimental results from Fig. 2c and 2d showed that the acquired

product exhibited maximum specific surface area(~164m^2/g) and pore volume(~0.598cm^3/g), when the

mixing speed was maintained 500 rpm at 403K for 18 h,
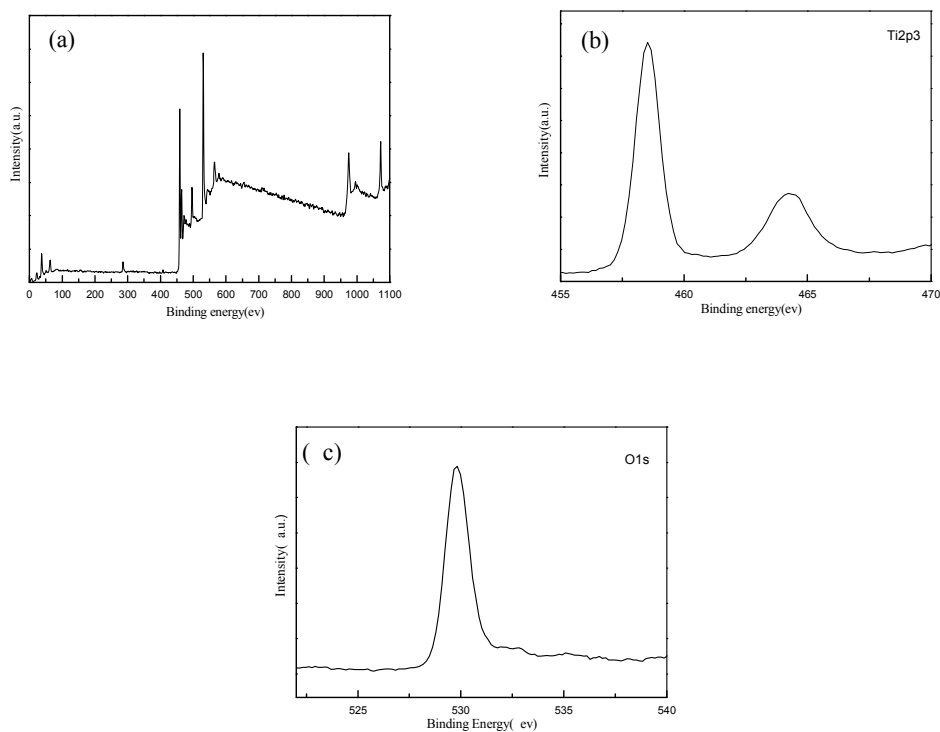
190

191

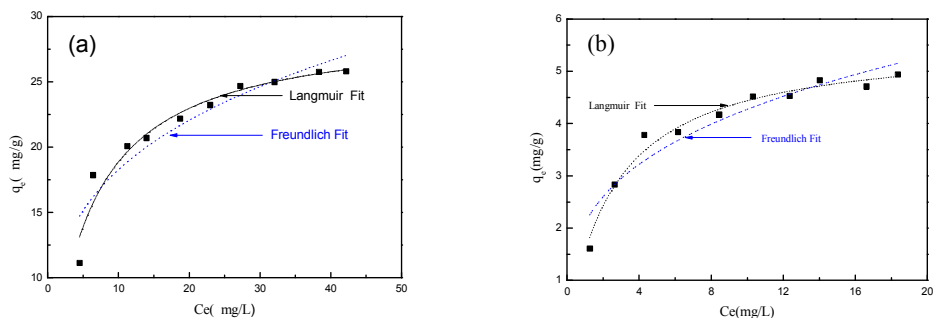Fig.3 XPS survey scans (a), the Ti2p3 deconvolution (b), and the O1s deconvolution (d) of TN.

As can be seen from Fig. 3b and Fig. 3c that binding energy of O1s was 529.5 ev, meantime, binding

energy of Ti_{2p3} were 458.5, 464.5ev, which were identical to the values of papers[31, 32], indicatingthe TN

still keep the same structure as TiO_2.

3.3 Adsorption isotherm

197

Fig. 4 Adsorption isotherms of CIP onto TN (a) and P25(b)

199

Table 1 Langmuir and Freundlich isotherms parameters of CIP onto P25 and TN (CIP concentration=10

201   mg/L, P25: 0.5 g/L; CIP concentration=25 mg/L, TN: 0.5 g/L)

| Adsorbent	Langmuir model			Freundlich model		
	K_L(l/mg)	q_m(mg/g)	R^2	K_F	1/n	R^2
P25	0.3830	5.597	0.9774	2.101	0.3083	0.8996
TN	0.1801	29.34	0.9436	9.782	0.2714	0.8780

202

203   The isotherms, as shown in Fig. 4, elucidated that the adsorption capacity of TN and P25 were 26.38

204   and 5.32 mg/g, respectively. The stronger adsorption capacity of TN was derived from high SSA and pore

205   volume (shown in Fig. 2c) (~50 m^2/g and 0.1cm^3/g) than P25. The fitting curves from Fig. 4 indicated

206   that Langmuir model was better fit the adsorption behaviors than the Freundlich model. The fitting results,

207   as listed in Table 1, showed that R^2 of Langmuir model on CIP adsorption onto P25 and TN were 0.97735

208   and 0.94364, respectively. This was attributed to less functional groups for the structures of P25 and TN.

209   Their adsorption behaviors mainly belonged to physical adsorption on themonomolecular layer[33].

210   3.4 The adsorption kinetic of CIP
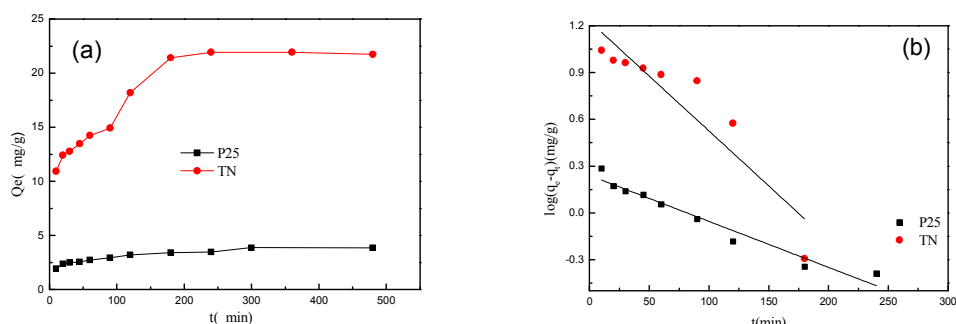
211
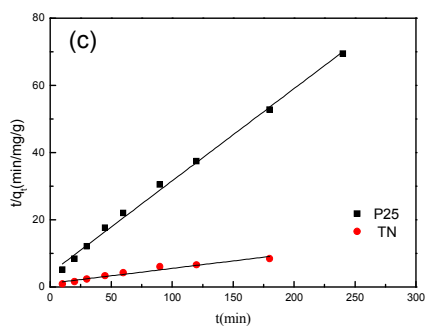
212

213   Fig. 5 Kinetic curves (a) of CIP adsorption onto P25 and TN (a) (the initial concentration of CIP was 25

214   and 50 mg/L, respectively); pseudo first-order model (R^2=0.9489, 0.8288)(b);

215   pseudo-second-ordermodel(c) (R^2=0.9965, 0.9473);

216   The equilibrium time of adsorption CIP onto P25 and TN can be obtained from Fig. 5a, they were 300

217   and 200 min, respectively. Physical and chemical effects of all the adsorption process involve the mass

218   transfer of a substance from the liquid phase to the adsorbent surface and form complex between CIP and

219   adsorbent. CIP solutions with 50 mg/L initial concentration were utilized to investigate the adsorption

220   kinetics of CIP on TN. The adsorption removal of CIP on TN was rapid and reach equilibrium in ~180

221   min. Besides, the change quantity ofconcentrationstep by step reduced due to the reduction of adsorption

222   sites onto TN during the adsorption process. However, the adsorption removal of CIP on P25 was slowly

223   and reached equilibrium in ~300 min. More equilibrium time was required for adsorption CIP onto P25

224   than TN, which may be attributed to the different pore structure of TN and P25.

225   Pseudo-first-order and Pseudo-second-order kinetic models[34, 35] were used to furtherinvestigat the

226   whole CIP adsorption process. Table 2 listed the kinetic parameters. The CIP sorption processes onto TN

227   and P25 were better fitted with the pseudo-second-order model by comparing the correlation coefficient

228   (R^2). The k_2 of CIP onto TN is bigger than that onto P25, which showed that TN represented a faster

229   adsorption speed than P25. Besides, the calculated q values (qe, cal) derived from the pseudo-second

230   model was more reliable than the pseudo-first model.

231   Table 2 Kinetic parameters of pseudo first- and second-order adsorption kinetic models for CIP on

232   anatase TN and P25. (CIP concentration=10 or 25 mg/L, TN or P25=0. 5 g/L)

Adsorbents	Initial conc.	$q_{e,exp}$	Pseudo first-order model			Pseudo second-order model		
	(mg/L)	(mg/g)	$k_1(min^{-1})$	$q_{e,cal}$	R^2	$k_2(min^{-1})$	$q_{e,cal}$	R^2
				(mg/g)			(mg/g)	
P25	5.0	26.28	0.0029	4.14	0.9489	0.0442	4.14	0.9965
TN	25	5.32	0.0070	22.2	0.8288	0.2746	22.2	0.9473

233   As shown in Fig. 5a，the TN represented faster adsorption speed and bigger adsorption capacity than

234   P25, which was attributed to larger SSA and pore volume of TN(shown in Fig. 2b). The mesoporous

235   characteristic of TN made the CIP diffuse faster into the pore canal of TN. The mesoporous characterisric

236   of TN is helpful for enhancing the photocatalytic process.

237   3.5 The regeneration properties of TN and P25
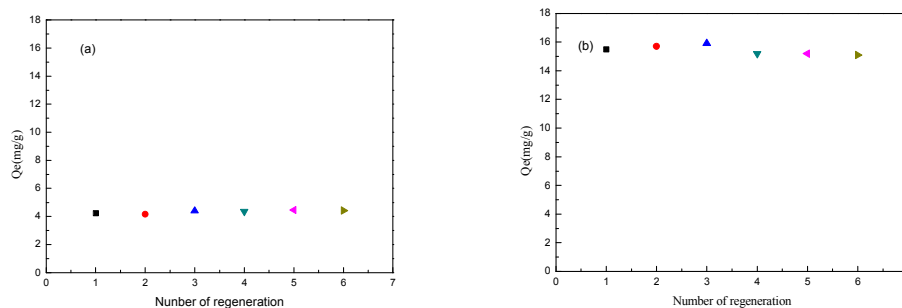
238

239   Fig. 6 The Regeneration of P25(a) (C_0=10mg/L) and anatase TN(b) (C_0=25mg/L)；

240   It can be observed that P25 and TN represented good regeneration capacity under UV light with a

241   500 W ultraviolet lamp for 3 h in 5 ml aqueous solution. This self-regeneration process can be recycled

242   more than 6 times with no decrease in adsorption capacity. The saturated sorption capacity can be kept at

243 ~16 mg/g from the sixth cycle after regeneration with a UV lamp, indicating that the adsorption

244 effectiveness of the TN adsorbent does not significantly change from the first cycle to the sith cycle.

Conclusion

246   In this paper, the long TiO_2 nanotubes were successfully prepared by reaction TiO_2 and NaOH using

247 a stirring hydrothermal method. The TN exhibiated outstanding adsorption performance due to its larger

248 SSA (~160 m^2/g) and pore volume (~0.6 cm^3/g) than those of commercial P25, and then it can be utilized

249 to efficiently adsorpt and remove the CIP from aqueous solution. The experimental results indicated TN

250 have excellent adsorption performance (26.38 mg/g) than P25 for the higher SSA. More importantly, TN

251 represented better regeneration properties after adsorption process, and then mineralize the pollutants.

252 This study provides a green method for the removal of organic pollutants by combining adsorption

253 enrichment with photocatalytic degradation.

254

259

Reference

261 1. S. Martin, A. Shchukarev, K. Hanna and J. F. Boily, *Environ Sci Technol*, 2015, **49**, 12197-12205.

262 2. P. L. M. TIAS PAUL, AND TIMOTHY J. STRATHMANN, *ENVIRONMENTAL SCIENCE & TECHNOLOGY*, 2007,

263 **41**, 8.

264 3. W. Q. Yulong Liao, Peng Zhong, Jin Zhang, and Yucheng He and E. Materials, *ACS Appl. Mater. Interfaces*, 2011, **3**,

265 4.

266 4. C. G. Daughton, *The Lancet*, 2002, **360**, 2.

267 5. D. K. F. Kolpin, E. T.; Meyer, M. T.; Thurman, M. E.; Zaugg, S. D.; Barber, L. B.; Buxton, H. T, *Environ. Sci.*

268 *Technol.*, 2002, **37**, 1.

269   6.   C. H. L. L. B. N. S. K. P. Y. K. Solomon, *Anal Bioanal Chem*, 2006, **384**, 9.

270   7.   L. H. Lissemore, C.; Yang, P.; Sibley, P. K.; Mabury, S. A.; Solomon, K. R, *Chemosphere*, 2006, **64**, 13.

271   8.   C. D. K. Metcalfe, B. G.; Bennie, D. T.; Servos, M.; Ternes, T. A.; Hirsch, R, *Environ. Toxicol. Chem*, 2003, **22**, 9.

272   9.   B. N. N. Halling-Sørensen, S.; Lanzky, P. F.; Ingerslev, F.; Holten   and H. C. J. Lutzhoft, S. E, *Chemosphere*, 1998,
273   **36**, 37.

274   10.   T. Heberer, *Toxicol. Lett.*, 2002, **131**, 13.

275   11.   O. A. H. V. Jones, N.; Lester, J. N., *Environmental Technology*, 2001, **22**, 12.

276   12.   K. Kümmerer, *Chemosphere*, 2001, **45**, 13.

277   13.   M. C. S. Dodd, A. D.; Gunten, U. V.; Huang, U. C.-H, *Environ. Sci. Technol.*, 2005, **39**, 12.

278   14.   Y. V. ico´, A, *Anal. Bioanal. Chem.*, 2007, **387**, 13.

279   15.   C. K. Gu, K. G., *Environ. Sci. Technol.*, 2005, **39**, 8.

280   16.   M. C. B. Dodd, M. O.; Gunten, U. V., *Environ. Sci. Technol*, 2006, **40**, 9.

281   17.   S. T. Kirsti Torniainen , Veikko Ulvi, *Int. J. Pharm.*, 1996, **132**, 9.

282   18.   C. C. ROBERTO ANDREOZZI，VINCENZO CAPRIO, MARCELLA DE CHAMPDOREÄ ,ROBERTO LO
283   GIUDICE,RAFFAELE MAROTTA, ANDETTORE ZUCCATO, *Environ. Sci. Technol*, 2004, **38**, 7.

284   19.   P. L. M. TIAS PAUL, AND TIMOTHY J. STRATHMANN, *Environ. Sci. Technol.*, 2007, **41**, 8.

285   20.   Y. M. Sun, J. H. Seo, C. J. Takacs, J. Seifter and A. J. Heeger, *Adv Mater*, 2011, **23**, 1679-+.

286   21.   C. W. Cheng, B. Liu, H. Y. Yang, W. W. Zhou, L. Sun, R. Chen, S. F. Yu, J. X. Zhang, H. Gong, H. D. Sun and H. J.
287   Fan, *Acs Nano*, 2009, **3**, 3069-3076.

288   22.   H. K. Yang, B. K. Moon, B. C. Choi, J. H. Jeong and K. H. Kim, *J Nanosci Nanotechno*, 2013, **13**, 6060-6063.

289   23.   L. Yang, M. Viste, J. Hossick-Schott and B. W. Sheldon, *Electrochim Acta*, 2012, **81**, 90-97.

290   24.   L. Y. Gong, X. H. Liu and L. H. Lu, *Mater Lett*, 2012, **67**, 226-228.

291   25.   K. F. Huo, X. M. Zhang, J. J. Fu, G. X. Qian, Y. C. Xin, B. Q. Zhu, H. W. Ni and P. K. Chu, *J Nanosci Nanotechno*,
292   2009, **9**, 3341-3346.

293   26.   X. T. a. D. Li, *Langmuir*, 2011, **27**, 6.

294   27.   Y. L. Liao, W. X. Que, P. Zhong, J. Zhang and Y. C. He, *Acs Appl Mater Inter*, 2011, **3**, 2800-2804.

295   28.   H. Kim, K. Noh, C. Choi, J. Khamwannah, D. Villwock and S. Jin, *Langmuir*, 2011, **27**, 10191-10196.

296   29.   T. Gao and B. P. Jelle, *J Phys Chem C*, 2013, **117**, 1401-1408.

297   30.   M. A. Behnajady, N. Modirshahla and H. Fathi, *J Hazard Mater*, 2006, **136**, 816-821.

298   31.   S. S. d. a. H. Siegbahn, *J. Phys. Chem. B*, 1997, **101**, 4.

299   32.   R. A. H. Bedri Erdem, Gary W. Simmons, E. David Sudol, Victoria L. Dimonie, and Mohamed S. El-Aasser,
300   *Langmuir*, 2001, **17**, 6.

301   33.   J. Ma, F. Yu, L. Zhou, L. Jin, M. Yang, J. Luan, Y. Tang, H. Fan, Z. Yuan and J. Chen, *ACS applied materials &*
302   *interfaces*, 2012, **4**, 5749-5760.

303   34.   R. M. Tinnacher, P. S. Nico, J. A. Davis and B. D. Honeyman, *Environmental science & technology*, 2013, **47**,
304   6214-6222.

305   35.   P. F. Salipante and S. D. Hudson, *Langmuir*, 2015.

306

307